New Developments and Challenges in Remote Sensing, Z. Bochenek (ed.)

Use of hyperspectral remote sensing to detect hazardous gas leakage from pipelines

H.M.A. van der Werff, M.F. Noomen, M. van der Meijde, J.F. Kooistra & F.D. van der Meer
International Institute for Geo-information Science and Earth Observation (ITC), Department of Earth Systems Analysis, Enschede, The Netherlands, Email: vdmeer@itc.nl

Keywords: pipeline, hydrocarbon, vegetation, stress, hyperspectral, spatial

ABSTRACT: Hydrocarbon leakage into the environment is a major problem with large economic and environmental impacts. Traditional methods for investigating seepage and pollution, such as drilling, are time- consuming, destructive and expensive. Remote sensing has proved to be a tool that offers a non-destructive investigation method and has a significant added value to traditional methods. Optical remote sensing has been extensively tested for exploration of onshore hydrocarbon reservoirs and detection of hydrocarbons at the Earth's surface. Theoretically, remote sensing is a suitable tool for direct and indirect detection of the presence of hydrocarbons in the environment. In this research we investigate a leaking pipeline through analysis of HyMap hyperspectral imagery. Due to inhomogeneous field cover, variations between fields turned out to be much larger than infield variations related to pollution issues. To overcome this problem a spatial-spectral normalization procedure was developed using moving kernels to enhance pollution related anomalies. The final results shows local anomalies which are likely related to hydrocarbon pollution.

1 INTRODUCTION

Hydrocarbon leakage into the environment is a major problem with large economic and environmental impacts. Hydrocarbon pollution can be either natural, through hydrocarbon seepage, or man-induced, through leaking pipelines or storage tanks. If a pipeline leak is large or undiscovered for a long time, substantial volumes of explosive gases in the soil can develop into dangerous situations involving costly remediation works. The United States National Transportation Safety Board (NTSB) has reported millions of dollars in losses and several casualties due to gas pipeline leaks in the recent years (NTSB 2001, 2003).

Traditional methods for investigating seepage and pollution, such as drilling, are time consuming, destructive and expensive. Remote sensing has proved to be a tool that offers a non-destructive investigation method and has a significant added value to traditional methods. Optical remote sensing has been extensively tested for exploration of onshore hydrocarbon reservoirs (e.g. Lang *et al.* 1984) and detection of hydrocarbons at the Earth's surface, (e.g. Li *et al.* 2005; Kühn *et al.* 2004; Hörig *et al.* 2001). Theoretically, remote sensing is a suitable tool for direct and indirect detection of the presence of hydrocarbon seepages (e.g. Noomen *et al.* 2005; Schumacher 2001;

Yang *et al.* 1998; Tedesco 1995). In practice, most of the observed geochemical and botanical anomalies that result from leaking hydrocarbons are subtle and not unique to pipeline leakage.

In the summer of 2004, a field campaign was performed to investigate the possible relationship between vegetation stress and hydrocarbon pollution resulting from leaking pipelines. The areas of interest were 4 meadows along a 1 km test trajectory. Based on the status of the vegetation interpreted from field spectral measurements, one field could be identified as being ''clean and healthy'' while two fields show a significant increase in vegetation stress directly above the pipeline (van der Meijde *et al.* 2004).

These results were confirmed by drilling records of 2003, which showed increased levels of benzene condensate in soil and ground water. As our sampling locations partly overlapped with these drilling locations, a comparison could be made between these two different measurement techniques. The general trend of the pollution levels, estimated from the drilling, appeared to be in strong agreement with anomalous regions in the vegetation health (van der Meijde *et al.* 2004). From 5 anomalous regions that had been found by drilling, 4 are overlapping with vegetation stress found by spectroscopic measurements.

As spectroscopy is capable of detecting botanical anomalies related to pipeline leakage, the use of air- or space borne hyperspectral imagery gives a good expectation. This research was consequently extended with the acquisition of airborne hyperspectral imagery. Not only would the need for expensive and time-consuming spectral field campaigns be reduced, it would also allow all fields to be simultaneously and consistently interpreted.

2 HYMAP HYPERSPECTRAL IMAGERY

An overflight with the HyMap airborne imaging spectrometer (Cocks *et al.* 1998) took place at the 19th of June 2005. Two field campaigns have been carried out in support of this flight. The first field campaign has been carried out in May 2005, at the beginning of the ''flight stand-by'' period and a month prior to the overflight. In this campaign, several meadows covered with grass have been measured with an ASD portable spectrometer. The purpose of these measurements was to obtain reference measurements for later comparison with the HyMap imagery. The second field campaign took place at the day of the overflight. The purpose of this campaign was to obtain bright and dark reference measurements of homogeneous surfaces, to assist in the calibration and validation of the HyMap imagery.

The dataset comprises two scenes that cover the entire 21 km length of the pipeline. The data was geometrically and atmospherically corrected by the German Aerospace Center (DLR) (Richter *et al.* 2002) and delivered in reflectance. In this paper, we concentrate on a test area along 1 km of the pipeline (Figure 1).

3 STANDARD PROCESSING TECHNIQUES

The processing of the HyMap imagery initiated with calculating the Normalized Difference Vegetation Index (NDVI, (Wessman *et al.* 1993)) (Figure 2), which expresses

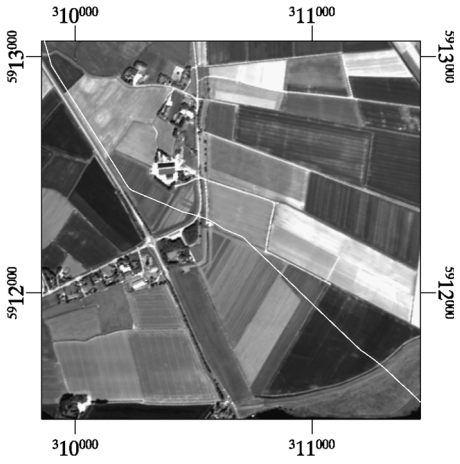

Figure 1. A natural colour composite of the Hymap imagery, showing the test area in the North of the Netherlands. The location of the pipeline is indicated by the NW-SE striking red line. The image dimensions are approximately 1600 × 1600 m.

the presence of vegetation in a scale of 0 to 1. Image pixels that are supposed to be influenced by land cover other than vegetation, such as buildings, roads and bare fields, were masked by an NDVI threshold of 0.6 DN. The spectral index that had been most successful in detecting spectral anomalies during the field campaigns is the red-edge position. This index represents the wavelength position of the red to near infrared intensity difference caused by chlorophyll, which is therefore typically found in vegetation spectra. The red-edge position was calculated after Guyot & Baret (1988) and

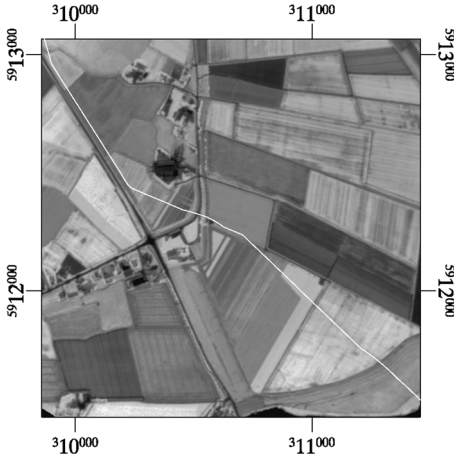

Figure 2. Normalized Difference Vegetation Index (NDVI) values calculated for the test area. The index ranges from 0 DN (black) to 1 DN (white) with a mean of 0.7 DN.

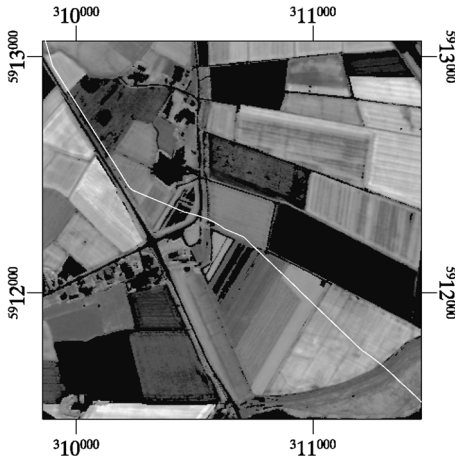

Figure 3. Rededge position calculated for the test area. The position of the rededge ranges from 715 nm (black) to 733 nm (white) with a mean of 722 nm. Pixels without sufficient vegetation cover are masked out by an NDVI threshold of 0.6 DN.

is based on four spectral bands in the visible and near-infrared wavelengths. As can be seen in Figure 3, the variation in red-edge position is mainly representing the variation between different fields rather than variation within a field. Studies of natural hydrocarbon seepages (Smith *et al.* 2004; Pysek & Pysek 1989; Hoeks 1983) showed that the influence of leaking hydrocarbons extends approximately 4 meters at maximum. Leakage from a pipeline is therefore expected to be seen as subtle spectral anomalies in the pixels that directly neighbour a leak. As the contrast in red-edge position in the HyMap image is mainly related to spectral differences between fields, a normalization procedure was necessary to enhance in-field variations.

4 NORMALIZATION PROCEDURE

A normalization procedure has been developed to correct for the variations in red-edge position between different fields. In this normalization procedure, the average value for a field is taken as the background value that represents its general state. A field is in this procedure defined as an homogeneous area with red-edge values that are within a 1 nm range from the pixel that is to be normalized. The normalization is done in a circular kernel that moves over the image. For each pixel, the reference value for the kernel is based on the 8 pixels that neighbour the central pixel (Figure 4). The central pixel that is to be normalized is excluded to avoid extreme pixel values from terminating the normalization process. The variance within the surrounding donut is not allowed to exceed the aforementioned threshold value of $+/-$ 1 nm with respect to the reference value. In case a certain pixel exceeds this threshold, it will not be taken into account in the calculations, with the result that the kernel will not incorporate pixels from fields with a different type of cover. This process is repeated for every pixel in the image. The

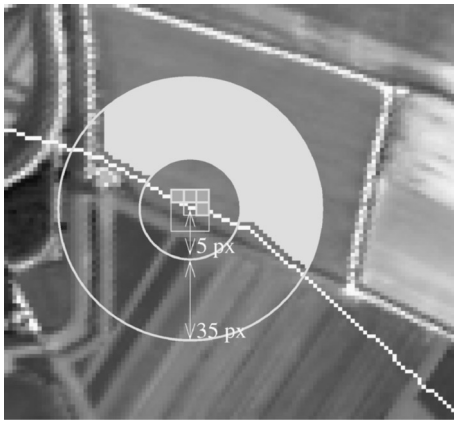

Figure 4. Schematic diagram of pixel normalization in a circular kernel. The centre pixel is ignored in the calculations, instead 8 neighbouring pixels are used to calculate a reference value. This reference value is compared with pixels in the yellow donut, which are used to calculate the background value of a field. In case a background pixel deviates more than 1 nm from the reference value, the kernel is assumed to be moving into another field, and the pixel is ignored in calculation of the background value. The 8 reference pixels and the surrounding kernel are not drawn to scale.

background values that are obtained by the moving kernel are shown in Figure 5. The separate fields got a homogenous background value, which indicates that the kernel represented the average background value for either field and was not exceeding into other fields. This automatically means that we established a background value that is almost equal for each pixel within a field.

The background values in Figure 5 are used to normalize each pixel in the red-edge image. Every pixel is scaled between -1 and $+1$ with respect to its background value. Values close to -1 mean that the red-edge is low with respect to the other pixels in the same field, and *vice versa*. Pixels with values that are close to 0 are close to the background value of a field. Figure 6 helps to assess whether this procedure is working properly. It can be observed that the pattern of red-edge values is scattered and that separate fields are not distinguishable anymore. This indicates that the normalization procedure has corrected for different vegetation types.

5 INTERPRETATION OF THE NORMALIZED IMAGE

Since every pixel in the image has been normalized, pixel values range between -1 and $+1$, where 0 is equal to the background value of a field. The interpretation therefore focuses on the negative values since these are pixels that are possible related to environmental problems. For representation of the vegetation health, a colour scale was chosen that ranges from green, representing relatively healthy vegetation with a value around 0, over yellow and orange to red, representing relatively stressed vegetation with

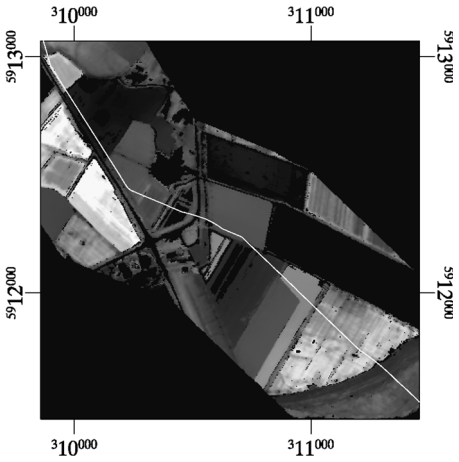

Figure 5. The background values for each pixel, calculated with the circular moving kernel. The values range from 717 nm (black) to 730 nm (white) with a mean of 722 nm. The values in each field are homogeneous while boundaries between these fields are sharp. This shows that the moving kernel approach can calculate the background value of a field and did not cross into other fields with a different spectral signature.

a value around −1. It is evident that not all anomalous vegetation is a result of environmental pollution. Many anomalies occur close to boundaries of fields or are related to in-field inhomogeneity such as worked tracks. However, by *a priori* knowledge of the location of the pipeline and by using the expected shape of anomalies, many anomalies can be ignored, which leaves only the anomalies that fulfill the defined

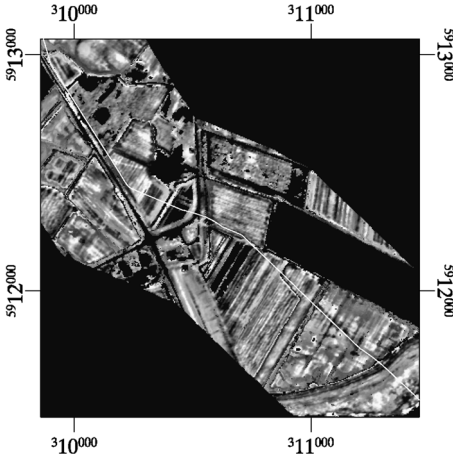

Figure 6. The normalized values for each centre pixel, calculated with the circular moving kernel. The values range from −0.81 DN (black) to 0.75 DN (white) with a mean of 0.0 DN.

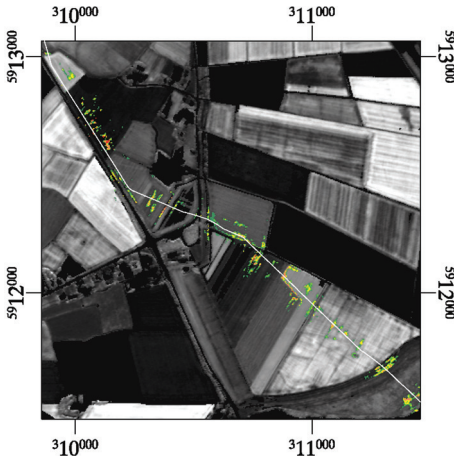

Figure 7. The interpreted anomalies shown on a natural colour composite of the HyMap image. Light green colours represent the normal (background) state of vegetation, while yellow, orange and red indicate areas with increased vegetation stress.

pattern of anomalies for interpretation. Anomalies further away from the pipeline are less likely to be caused by processes related to the pipeline. Every pixel was weighted with respect to its distance from the pipeline. Figure 7 shows the result after the weighing process. Anomalies further away from the pipeline are now suppressed what improves the visibility of anomalies close to the pipeline.

6 DISCUSSION AND CONCLUSIONS

In this research, we developed a method for image normalization which visualized in-field variations rather than variation between fields. In the intermediate steps of the image processing, one can clearly observe the functionality of the algorithm to derive so-called background values for each separate field in the image.

The normalization procedure resulted in clustering of anomalies in the image. Some of these clusters occurred relatively far away from the pipeline and are therefore not likely to be related to pipeline leakage. The addition of another spatial criterion, limiting the occurrence of anomalies to the direct environment of the pipeline, resulted in a cleaned image. In this cleaned image, only those anomalies that fall within a certain buffer of the pipeline are shown. It is important to realize that not every anomaly is necessarily related to the pipeline. There is a certain natural variance in the vegetation that occasionally might appear as a potential pollution anomaly.

In the expert analysis, we tried to avoid the interpretation of natural variance as pipeline related anomaly. Using spatial (relative spatial occurrence of anomalies with respect to the whole field) and spectral criteria we attempted to minimize the amount of false anomalies in our interpretation. It needs to be stressed that there is no proper way to assess the success rate of our interpretation without ground truth information.

In the test area, only two fields were in a good enough condition to be evaluated. Unfortunately, no ground truth information was available on these two meadows. Because of unfortunate mowing regimes of the farmers and delay in the acquisition of the airborne measurement due to military airspace restrictions there was no comparison possible with the field data obtained prior to the flight. As the step from field spectra information to image spectral information involves a spatial mixing of signals, the existing ground truth information could not be used for image processing. The success rate of our interpretation is likely to increase when additional ground truth information becomes available for areas that were well vegetated at the moment of overflight. The development of an automatic procedure will depend on the validation of our present results and a subsequent tuning of the processing method.

REFERENCES

Abrams, M., Conel, J., Lang, H. & Paley, H. (Eds.) 1984. *The joint NASA / Geosat Test Case Project*, Volume 1. Tulsa, Oklahoma, USA: The American Association of Petroleum Geologists (AAPG).

Cocks, T., Jenssen, R., Stewart, A., Wilson, I. & Shields, T. 1998. The HyMap airborne hyperspectral sensor: the system, calibration and performance. In M Schaepman, D Schläpfer, and K Itten (Eds.), *Proceedings of the 1st EARSeL workshop on Imaging Spectroscopy, 6–8 October 1998, Zürich, Switzerland*, Remote Sensing Laboratories, University of Zürich, Switzerland, pp. 37–42.

Guyot, G. & Baret, F. 1988. Utilisation de la haute resolution spectrale pur suivre l'etat des couverts vegetaux. In *Proceedings of the 4th International Colloquium on Spectral Signatures of Objects in Remote Sensing, Aussios, France, 18–22 January 1988*, ESA SP-287, pp. 279–286.

Hoeks, J. 1983. Gastransport in de bodem. Technical report, Instituut voor cultuurtechniek en waterhuishouding, Wageningen, The Netherlands.

Hörig, B., Kühn, F., Oschütz, F. & Lehmann, F. 2001. Hymap hyperspectral remote sensing to detect hydrocarbons. *International Journal of Remote Sensing* 22(8), 1413–1422.

Kühn, F., Oppermann, K. & Hörig, B. 2004. Hydrocarbon index – an algorithm for hyperspectral detection of hydrocarbons. *International Journal of Remote Sensing* 25(12), 2467–2473.

Lang, H., Aldeman, W. & Sabins Jr., F. 1984. *Patrick Draw, Wyoming – petroleum test case report.*, pp. 11–1 – 11–28. Volume 1 of Abrams *et al*, 1984.

Li, L., Ustin, S. & Lay, M. 2005. Application of AVIRIS data in detection of oil-induced vegetation stress and cover change at Jornada, New Mexico. *Remote Sensing of Environment* 94, 1–16.

Noomen, M., van der Meer, F. & Skidmore, A. 2005. Hyperspectral remote sensing for detecting the effects of three hydrocarbon gases on maize reflectance. In *Proceedings of the 31st international symposium on remote sensing of environment: global monitoring for sustainability and security*, St. Petersburg, Russia.

NTSB, 2001. Natural gas exploitation and fire in South Riding, Virginia, July 7, 1998. Technical report, National Transportation Safety Board, Washington D.C. p. 27.

NTSB, 2003. Natural gas pipeline rupture and fire near Carlsbad, New Mexico. Technical report, National Transportation Safety Board, Washington D.C. p. 57.

Pysek, P. & Pysek, A. 1989. Veränderungen der vegetation durch experimentelle erdgasbehandlung. *Weed Research* 29, 193–204.

Richter, R., Müller, A. & Heiden, U. 2002. Aspects of operational atmospheric correction of hyperspectral imagery. *International Journal of Remote Sensing* 23(1), 145–157.

Schumacher, D. 2001. Petroleum exploration in environmentally sensitive areas: Opportunities for non-invasive geochemical and remote sensing methods. pp. 012–1–012–5., Annual Convention of the ASPG.

Smith, K., Steven, M. & Colls, J. 2004. Use of hyperspectral derivative ratios in the red-edge region to identify plant stress responses to gas leaks. *Remote sensing of environment* 92, 207–217.

Tedesco, S. 1995. *Surface geochemistry in petroleum exploration*. New York: Chapmann & Hall.

van der Meijde, M., van der Werff, H. & Kooistra, J. 2004, 13–17. Detection of spectral features of anomalous vegetation from reflectance spectroscopy related to pipeline leakages. In *Proceedings of SPIE*, San Francisco. American Geophysical Union.

Wessman, C., Bateson, C., Curtiss, B. & Benning, T. 1993. A comparison of spectral mixture analysis and ndvi for ascertaining ecological variables. In R Green (Ed.), *Summaries of the Fourth Annual JPL Airborne Geoscience Workshop, 25–29 October 1993*, *Volume 1. Aviris Workshop, JPL Publication 93–26, Vol.1*, Pasadena, California: NASA, Jet Propulsion Laboratory, pp. 193–196.

Yang, H., Zhang, J., van der Meer, F. & Kroonenberg, S. 1998. Geochemistry and field spectrometry for detecting hydrocarbon microseepage. *Terra Nova* 10(5), 231–235.